

Fusobacterium Nucleatum Aggravates Intestinal Barrier Impairment and Colitis Through IL-8 Induced Neutrophil Chemotaxis by Activating Epithelial Cells

Zhiyue Wang^{1,2,*}, Bowen Li^{1,2,*}, Liqing Bao^{1-3,*}, Yu Chen^{1,2}, Jinhua Yang^{1,2}, Fangqi Xu¹⁻³, Shang Shi⁴, Wanlu Chen^{2,5}, Boding Wang^{2,5}, Yang Liu^{1,2}

¹Department of Pancreatic and Gastrointestinal Surgery Division, Ningbo No.2 hospital, Ningbo, People's Republic of China; ²Ningbo Key Laboratory of Intestinal Microecology and Human Major Diseases, Ningbo, People's Republic of China; ³Department of Cixi Biomedical Research Institute, Wenzhou Medical University, Ningbo, People's Republic of China; ⁴Department of Breast Surgery, Ningbo Medical Center Lihuli Hospital, Ningbo, People's Republic of China; ⁵Department of Neurosurgery, Ningbo No.2 hospital, Ningbo, People's Republic of China

*These authors contributed equally to this work

Correspondence: Yang Liu; Boding Wang, Email lyang712@icloud.com; wangboding06@126.com

Background: Inflammatory bowel disease (IBD) is affected by interactions between intestinal microbial factors, abnormal inflammation, and an impaired intestinal mucosal barrier. Neutrophils (NE) are key players in IBD. *Fusobacterium nucleatum* (*F. nucleatum*) is reported to contribute to IBD progression. However, the relationship between *F. nucleatum*, abnormal inflammation, and intestinal barrier impairment should be interpreted to understand the role of *F. nucleatum* in IBD.

Methods: Dextran sulfate sodium (DSS)-induced colitis model was established and mice were orally administered with *F. nucleatum*. *F. nucleatum* colonization was confirmed by fluorescence in situ hybridization (FISH) and PCR. Intestinal barrier impairment was investigated by tight junction protein expression. Immuno-histochemistry (IHC) for Ly6G and flow cytometry detection to measure NE chemotaxis in mouse colon tissues. Caco-2 monolayers were used to evaluate epithelial integrity and permeability in vitro. A transwell model involving caco-2 cells and NE co-culture was used to assess NE chemotaxis. NE chemokines were measured by ELISA. A mouse model of NE exhaustion using an anti-Ly6G antibody was used to identify the role of NEs in *F. nucleatum*-induced colitis. Transcriptome sequencing and bioinformatics analysis were applied to screen cytokines and signaling pathways.

Results: Administration of *F. nucleatum* aggravated colitis in the DSS model. *F. nucleatum* infection downregulates ZO-1 and Occludin expression and increases intestinal permeability. Additionally, *F. nucleatum*-induced NE chemotaxis decreases the integrity and permeability of the caco-2 monolayer. *F. nucleatum*-induced NE chemotaxis is dependent on IEC-derived interleukin 8 (IL-8) secretion, mediated by the TLR2/ERK signaling pathway. In addition, NE exhaustion in mice inhibited *F. nucleatum*-induced intestinal barrier impairment and colitis.

Conclusion: *F. nucleatum* improves NE chemotaxis by infecting intestinal epithelial cells (IECs) to secrete IL-8 and aggravate intestinal barrier impairment, contributing to the progression of intestinal inflammation. Examining and eliminating *F. nucleatum* could be a valuable microbiome-based method for IBD surveillance and prevention.

Keywords: inflammatory bowel disease, IBD, *Fusobacterium nucleatum*, neutrophil chemotaxis, IL-8, intestinal barrier impairment

Introduction

Inflammatory Bowel Disease (IBD) is a group of inflammatory conditions affecting the intestine and is characterized by symptoms, such as diarrhea, abdominal pain, mucus, pus, and bloody stools, accompanied by varying degrees of extraintestinal manifestations. IBD is primarily categorized into ulcerative colitis (UC) and Crohn's Disease.^{1,2} With increasing incidence and disease complications, IBD has emerged as a significant threat to human health. IBD arises from

a convergence of genetic, environmental, and microbial factors, each necessary but insufficient alone to cause the disease.¹ The potential significance of the microbiota in the development, progression, and treatment of IBD is becoming a subject of considerable interest.

Recent studies have revealed that highly abundant *F. nucleatum* colonizes the intestinal tissues of IBD patients, suggesting *F. nucleatum* is tightly linked to IBD development.^{3,4} Further studies have shown that *F. nucleatum* contributes to the progression of IBD by regulating inflammation.⁵ Neutrophils (NEs) infiltrate inflammatory cells in IBD, releasing reactive oxygen species (ROS) and proteases and resulting in intestinal barrier impairment.⁶ Dysfunction of the intestinal barrier allowing pathogens to pass through the mucosal layer enhances direct contact between the microbiota and epithelial cells, as well as increases contact with NEs in the lamina propria.⁷ Typically, NEs are anti-pathogen performers that can be activated by gut microbiota, such as *F. nucleatum*. It has been reported that *F. nucleatum* infection induces NE infiltration and MMP-9 secretion, leading to distortion of colon tissue.⁸ However, whether *F. nucleatum* induces NE chemotaxis and contributes to IBD progression should be interpreted.

In this study, we investigated the relationship between *F. nucleatum* and NEs in the colitis mice model and in vitro. Our results demonstrated that *F. nucleatum* aggravated intestinal inflammation and barrier impairment by inducing NE chemotaxis mediated by IECs-derived IL-8. These findings provide valuable insights into effective diagnosis and clinical management of IBD.

Materials and Method

Cells Culture

The human colonic epithelial cell caco-2 was purchased from the National Collection of Authenticated Cell Cultures and cultured in DMEM (Vivacell, Germany) supplemented with 20% fetal bovine serum (Gibco, USA) at 37°C and 5% CO₂.

Bacterial Strains

F. nucleatum strain ATCC25586 was acquired from the American Type Culture Collection (ATCC, Manassas, VA, USA) and cultivated overnight at 37°C under anaerobic conditions in brain–heart infusion (BHI) supplemented with hemin, K₂HPO₄, and vitamin K1.

DSS-Induced Mouse Model of Colitis

Six-week-old male C57BL/6J mice were purchased from Charles River and used for all experiments. Twenty mice were randomly and evenly assigned to the Control, DSS, *F. nucleatum*, and DSS + *F. nucleatum* groups. The body weights of the mice were measured and feces were collected daily to calculate the disease activity index (DAI). At the beginning of the experiment, mice were treated with 2.5% dextran sulfate sodium (DSS; 40kDa, Macklin, China) mixed with drinking water to establish a colitis model, except for the Control and *F. nucleatum* groups. In addition, in the *F. nucleatum* and DSS+ *F. nucleatum* group, mice were given 100ul *F. nucleatum* suspension (10⁹CFU/mL) by gavage once a day for seven days, then sacrificed for further studies. For each day, the mean disease activity index (DAI) was calculated according to the standard applied by Katerina et al.⁹ The experimental procedures were approved by the Ethics Review Committee of Guoke Ningbo Life Science and Health Industry Research Institute (GK-2022-12-031) and performed following Regulations for the Administration of Affairs Concerning Experimental Animals in Zhejiang Province and Laboratory animals–General requirements for animal experiment.

Neutrophil Isolation

Fresh mouse intestinal tissue was prepared in a single-cell suspension using Liberase (Roche, Switzerland) and DNase I (Roche, Switzerland). NEs were isolated by gradient centrifugation using different ratios of precools (Sigma-Aldrich, USA).

Neutrophil Exhaustion

Mice were injected intraperitoneally with 350 μg of anti-Ly6G (clone1A8, Bickel, Catalog. BE0075-1) antibodies on the first day and fourth day. Ly6G⁺ cell exhaustion was confirmed by harvesting spleens from a subset of mice and subsequently analyzing them using flow cytometry after one week.

Neutrophil Migration Assay

NEs (2.5×10^5 /well) were introduced into the upper chamber of the Transwell system (8.0 μm pore size; Falcon), whereas *F. nucleatum* (1.0×10^8 CFU/well) and caco-2 cells (1.0×10^6 /well) were introduced into the lower chamber. After a few hours, the upper chamber was detached and the cells were fixed using methanol. Subsequently, the cells on the membrane were stained with a crystal violet solution, photographed, and quantified.

Flow Cytometry

The isolated NEs were washed with flow cytometry staining buffer to dissociate them into single cells. To identify NEs, the cells were stained with FITC-labeled anti-Ly6G Mba (BioLegend, USA), PE-labeled anti-Ly6C Mba (BioLegend, USA), and APC-labeled anti-CD11b Mba (BioLegend, USA), respectively. After 15 min of staining, the cells were washed twice with the staining buffer. After washing, the percentage of Ly6G⁺ cells was immediately examined using flow cytometry.

Histological Staining

Following hematoxylin and eosin (H&E) staining of tissue sections, histological scores were assessed by three independent pathologists. The histological scores were determined blindly as follows: Damaged area: 0: n/a, 1: $\leq 25\%$, 2: $\leq 50\%$, 3: $\leq 75\%$, 4: $\leq 100\%$. Muco-depletion of glands: 0 = none, 1 = mild, 2 and 3 = moderate, 4 = severe. Tissue damage: 0 = no mucosal damage, 1 = discrete epithelial lesions, 2 = surface mucosal erosion or focal ulceration, 3 = extensive mucosal damage and extension into deeper structures of the bowel wall. Inflammatory cell infiltration: 0 = occasional inflammatory cells in the lamina propria, 1 = increased numbers of inflammatory cells in the lamina propria, 2 = confluence inflammatory cells, extending into the submucosa, 3 = transmural extension of the infiltrate. The total histopathological score was determined by summation of the scores from each category.

Immunohistochemistry

Immunohistochemistry (IHC) for occludin, ZO-1, TLR2, and Ly6G was performed using colon sections obtained from a mouse model of colitis. After dewaxing, rehydration, and PBS washing, the sections were antigen retrieval in 0.5M EDTA buffer (pH 8.0) (Solarbio, China). The following steps were conducted using an Ultrasensitive SP kit (Maxim Biotechnologies, China) following the manufacturer's protocol. Cells were incubated with antibodies against occludin, ZO-1, TLR2, and Ly6G at four degrees overnight. Finally, the sections were photographed under a light microscope at magnifications of 100 \times and 200 \times .

Fluorescence in situ Hybridization (FISH)

A Cy3- conjugated *F. nucleatum* 16S rRNA probe (5'-CTT GTA GTT CCG C(C/T) TAC CTC-3') was used for the FISH assay to detect the existence of *F. nucleatum*.¹⁰ The dewaxed and rehydrated paraffin tissue sections were treated with proteinase K and fixed with 1% paraformaldehyde, then incubated with the pro-hybridized buffer for 3h at 37°C. A mixture of hybridization buffer and the probe was used to incubate the sections for 18h in a dark chamber at 42°C. After counterstaining with DAPI, the images were captured with a fluorescence microscope.

The Caco-2 Transwell System

The transwell system was used to coculture NEs and caco-2 cells. To investigate the influence of NEs on caco-2 monolayer, caco-2 cells (5.0×10^5 /well) were seeded as a monolayer on a polycarbonate membrane inserted into the transwell system (0.4 μm pore size; Falcon). After transepithelial resistance of the caco-2 monolayer reached 300 $\Omega \cdot \text{cm}^2$,

NEs (1.0×10^6 /well) were introduced into the lower chamber. After several hours, cells and supernatants were harvested for further analysis.

Fluorescein Isothiocyanate Transmittance Detection

A freshly prepared solution of fluorescein isothiocyanate-labeled dextran (FITC-dextran; FD4; 4kDa; Sigma, USA) dissolved in HBSS (1 mg/mL) was introduced into the upper chamber. After incubation at 37°C for 2 h, a specific volume of culture medium was retrieved from the lower chamber and the fluorescence intensity (excitation 485 nm, emission 525 nm) was measured using a fluorescence enzyme labeling instrument (Molecular Devices, USA).

Measurement of Transepithelial Resistance

Caco-2 cells, seeded into transwell upper chambers (5.0×10^5 /well), were used to assess the transepithelial cell resistance of the intestinal epithelial barrier using the Millicell-ERS system (Millipore, USA). Two transwells containing only the culture medium were designated as blank controls, and the entire measurement process was conducted at a constant temperature. Each transwell was assessed three times in three different directions, and the average value was used to determine the transepithelial electrical resistance (TEER), expressed in $\Omega \cdot \text{cm}^2$. $\text{TEER} = (\text{measured TEER} - \text{blank pore TEER}) \times \text{effective membrane area of the cell culture compartment}$.

Transcriptome Sequencing and Bioinformatics Analysis

Inoculate caco-2 cells from the logarithmic growth phase into a 6-well plate, with 1×10^6 cells per well, and culture for 24h. Suspend the calculated number of *F. nucleatum* in DMEM medium and co-culture with a ratio of 100:1 for 4 h to construct an infection model. Total RNA was isolated using Trizol reagent (Invitrogen). The RNA-seq transcriptome library was prepared using the TruSeq™ RNA sample preparation Kit from Illumina (San Diego, CA), following the manufacturer's instructions, using 1 μg of total RNA. The library was then quantified using TBS380, and a paired-end RNA-seq sequencing library was created and sequenced with the Illumina HiSeq xten/NovaSeq 6000 sequencer ($2 \times 150\text{bp}$ read length). Differential expression analysis was performed using DESeq2, DEGs with $|\log_2\text{FC}| > 1$, and a p-value ≤ 0.05 were considered significantly different expressed genes. In addition, bioinformatics analysis was performed including Gene Ontology (GO) and Kyoto Encyclopedia of Genes and Genomes (KEGG).

Rt-Pcr

Total RNA was isolated using Trizol reagent (Invitrogen), and 1 μg of total RNA was reverse-transcribed using the ReverTra Ace® qPCR RT Master Mix with gDNA Remover (Toyobo, Japan). Real-time quantitative PCR (qPCR) was performed using a Genomic DNA Purification Kit (Tiangen, China). The Ct values obtained from different samples were compared using the $2^{-\Delta\Delta\text{Ct}}$ method. Glyceraldehyde-3-phosphate dehydrogenase (GAPDH) served as an internal reference transcript. The primers used are listed in Table 1.

Table 1 RT-qPCR Primers Were Used in the Study

Name	Sequence 5'-3'
GAPDH Human	F: TGTGGGCATCAATGGATTTGG R: ACACCATGTATTCCGGGTCAAT
GAPDH Mouse	F: AATGGATTTGGACGCATTGGT R: TTTGCACTGGTACGTGTTGAT
Occludin Human	F: ACAAGCGGTTTTATCCAGAGTC R: GTCATCCACAGGCGAAGTTAAT

(Continued)

Table 1 (Continued).

Name	Sequence 5'-3'
Occludin Mouse	F: TGAAAGTCCACCTCCTTACAGA R: CCGGATAAAAAGAGTACGCTGG
ZO-1 Human	F: CAACATACAGTGACGCTTCACA R: CACTATTGACGTTTCCCCACTC
ZO-1 Mouse	F: GCTTTAGCGAACAGAAGGAGC R: TTCATTTTTCCGAGACTTCACCA
IL-8 Human	F: ACTGAGAGTGATTGAGAGTGGAC R: AACCTCTGCACCCAGTTTTTC
<i>F. nucleatum</i> 16S rRNA	F: CGGGTGAGTAACGCGTAAAG R: ACATTGTGCCACGGACATCTTG
Bacterial universal 16S rRNA	F: GTGSTGCAYGGYTGTCGTCA R: ACGTCRTCCMCACCTTCCC

Western Blotting (WB)

Total cellular protein was isolated from cultured cells and mouse colons using a protein extraction solution (Beyotime, China). The proteins were separated by 10% and 12% sodium dodecyl sulfate-polyacrylamide gel electrophoresis (SDS-PAGE) and transferred to polyvinylidene fluoride (PVDF) membranes at 300 mA for two hours at four degrees, utilizing a wet-blotting apparatus (Bio-Rad). The membranes were blocked with 5% non-fat milk for an hour at room temperature and then incubated overnight at four degrees with primary antibodies diluted in TBST. Subsequently, the membranes were incubated with appropriate secondary antibodies for 1 h at room temperature. Protein signals were detected using the ChemiDoc™ XRS+ system (Bio-Rad). The following primary antibodies were used for WB: ZO-1 (Proteintech), occludin (Proteintech), β -actin (Proteintech), TLR2 (Abcam), ERK (Proteintech), and p-ERK (Proteintech).

Statistical Analysis

Statistical analysis was performed using Prism 8.4.2 software, and data from at least three independent experiments are expressed as the mean \pm standard error (SE). Error bars in the scatterplots and bar graphs represent SE. The differences were considered significant at * $p < 0.05$, ** $p < 0.01$, *** $p < 0.001$.

Results

F. Nucleatum Impairs the Intestinal Barrier and Aggravates DSS-Induced Colitis

A mouse model of DSS-induced colitis was established to explore the effect of *F. nucleatum* on colitis in vivo and explore the underlying mechanism (Figure 1A). We confirmed that *F. nucleatum* successfully colonized the mice intestines following oral administration (Figure 1B and C). We observed that *F. nucleatum* treatment led to body weight loss and shortening of colon length. In addition, *F. nucleatum* increased disease activity index (DAI) score in mice (Figure 1D–F). *F. nucleatum* also augmented mucosal necrosis and inflammatory cell infiltration, exacerbating colitis severity (Figure 1G). In addition, we observed increased serum FD4-fluorescein levels in *F. nucleatum*-treated mice (Figure 2A). In addition, the expression of ZO-1 and Occludin decreased in *F. nucleatum*-treated mice (Figure 2B–D). These results demonstrated that *F. nucleatum* infection exacerbates intestinal barrier impairment.

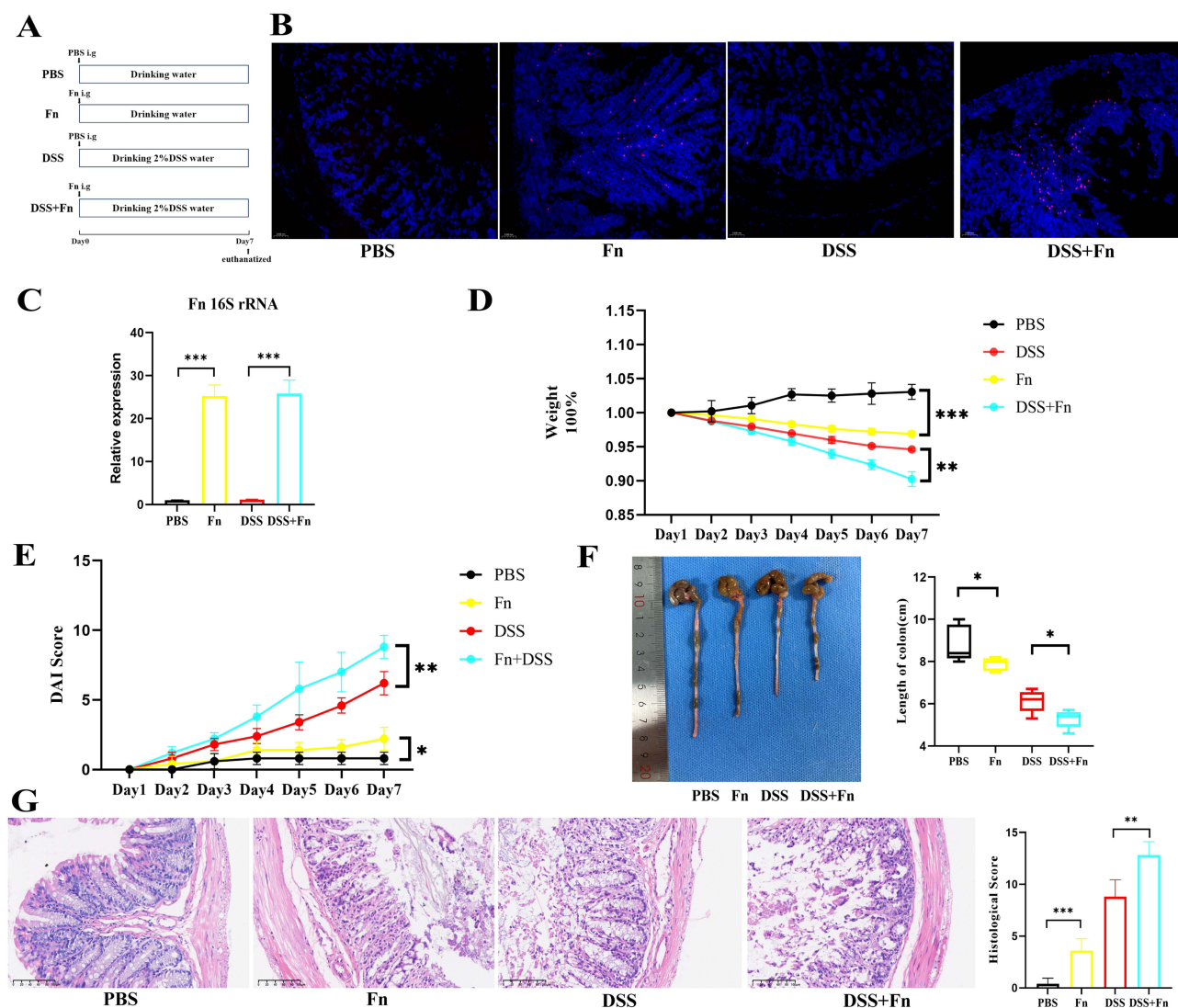


Figure 1 *F. nucleatum* aggravates DSS-induced colitis. (A) Experimental design outlining the DSS-induced colitis mice model and *F. nucleatum* treatment protocol. (B) Representative *F. nucleatum* 16S rRNA (red) FISH staining of mouse colon, nuclei were stained blue using DAPI (blue). Scale bar = 50 μ m. (C) Relative abundance of *F. nucleatum* in colon tissues were calculated by RT-qPCR. (n = 5 mice per group) (D) Effect of *F. nucleatum* on the body weight of DSS-treated mice. (n = 5 mice per group) (E) Clinical DAI was assessed following DSS exposure. (n = 5 mice per group) (F) A Photograph of the representative colon and colon length was measured on day 7 after colitis induction. (n = 5 mice per group) (G) Representative H&E staining of colon sections and histological score of the staining on day 7 after colitis induction. Scale bar = 100 μ m. (n = 5 mice per group) * p <0.05, ** p <0.01, *** p <0.001. All data are presented as mean \pm SD.

Abbreviations: PBS, phosphate-buffered saline; DSS, dextran sulfate sodium; DAI, disease activity index; H&E, hematoxylin and eosin.

F. Nucleatum Infection Contributes to Neutrophils Chemotaxis Inducing Intestinal Barrier Impairment

Next, we evaluated the relationship between NE chemotaxis and *F. nucleatum*. We found that NE infiltration was higher in the intestinal tissue of the *F. nucleatum* group (Figure 3A). In addition, the proportion of Ly6G-positive cells in the *F. nucleatum* group was also higher (Figure 3B). IEC-induced chemokine secretion is a typical mechanism for NE infiltration in IBD. To demonstrate the necessity of IECs in *F. nucleatum* to induce NE chemotaxis, we verified this using the Transwell model in vitro (Figure 3C). We found that *F. nucleatum*-infected caco-2 cells attracted more NEs than caco-2 or *F. nucleatum* alone (Figure 3D), indicating that *F. nucleatum*-infected IECs are necessary for NE chemotaxis. To further investigate the contribution of NE chemotaxis to intestinal barrier integrity and permeability, caco-2 cells were cultured on a permeable filter to form a monolayer that mimicked the intestinal epithelial barrier. We evaluated epithelial integrity and permeability by measuring TEER and FD-4 flux (Figure 3E). We found that *F. nucleatum* infection did not

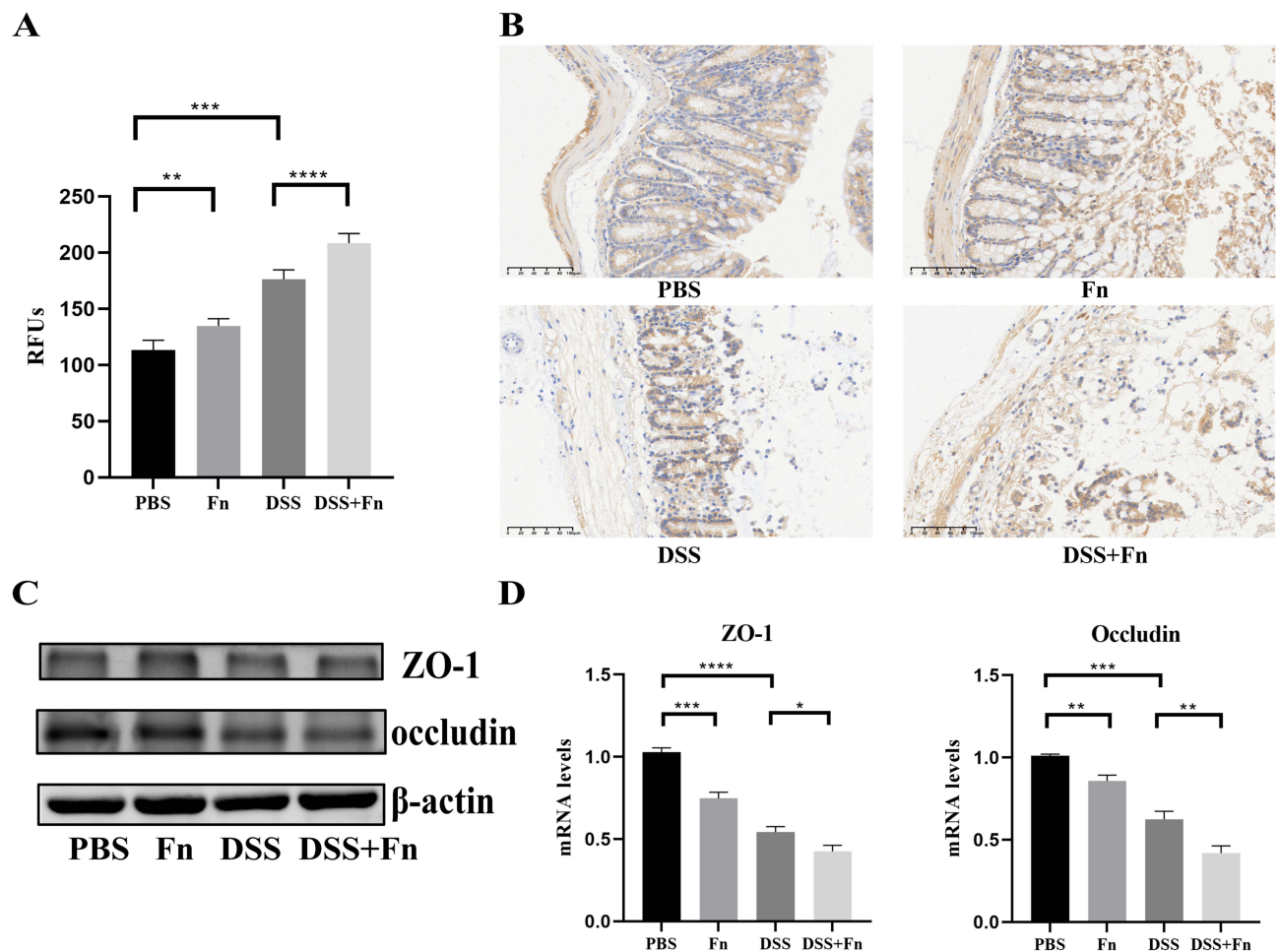


Figure 2 *F. nucleatum* aggravates the intestinal barrier impairment. (A) Relative fluorescence intensity of FITC-Dextran 4kDa in blood 2 hours after oral administration of FD4. (n = 5 mice per group) (B) Representative images of immunohistochemical staining of occludin in the colon on day 7 after colitis induction. Scale bar = 100 μ m. (C) Immunoblot analysis of protein extracts from colon samples with the indicated antibodies. (D) The relative mRNA level of ZO-1 and occludin was detected in colon samples on day 7 after colitis induction. (n = 5 mice per group). * p <0.05, ** p <0.01, *** p <0.001, **** p <0.0001. All data are presented as mean \pm SD.

significantly affect the integrity or permeability of the caco-2 monolayer barrier. However, when NEs were added to the lower chamber, a persistent decrease in TEER and an increased FD4 flux in the *F. nucleatum* infected group were observed (Figure 3F and G), suggesting that NEs contributed to intestinal barrier impairment.

Epithelial Cells Were Activated by *F. Nucleatum* to Secrete IL-8 and Then Recruiting Neutrophils

To explore the factors leading to NE chemotaxis, we performed transcriptome analysis of *F. nucleatum*-infected epithelial cells and found a series of upregulated NE chemoattractant chemokines, with the most significant increase observed in IL-8 expression (Figure 4A). We then confirmed the increase in IL-8 expression by RT-PCR and ELISA (Figure 4B and C). To confirm the role of IL-8 in NE chemotaxis, we used Reparixin, an IL-8 receptor inhibitor, and found that NE chemotaxis was significantly inhibited (Figure 4D). We further investigated this effect on caco-2 cell monolayers infected with *F. nucleatum* and found a decrease in TEER after Reparixin application (Figure 4E). Meanwhile, a decrease in FD-4 flux also indicated restoration of intestinal barrier function when Reparixin was applied (Figure 4F). These results suggested that NE chemotaxis depends on IECs-derived IL-8 after *F. nucleatum* infection.

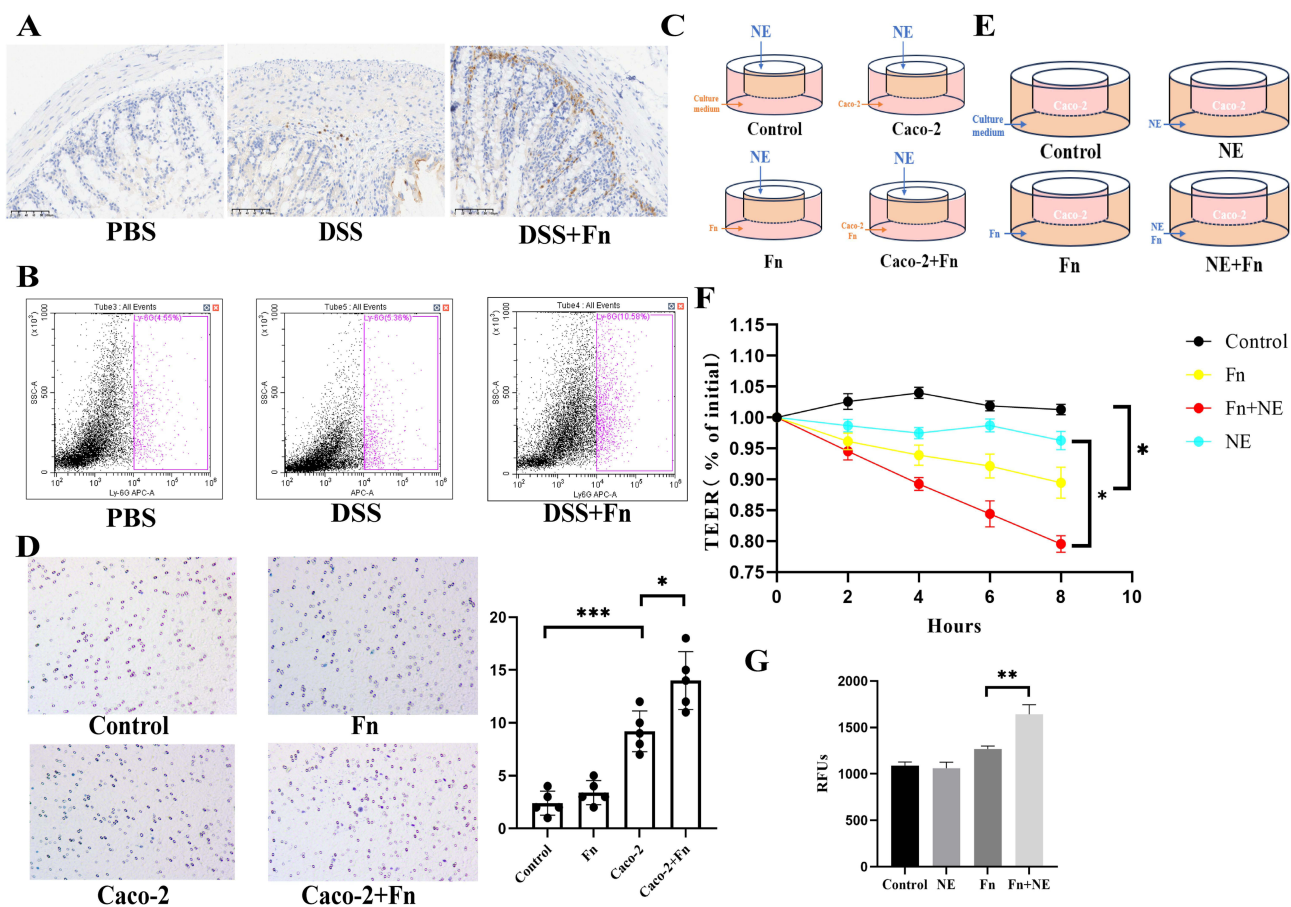


Figure 3 *F. nucleatum* infection contributes to neutrophils chemotaxis inducing intestinal barrier impairment (A) Representative images of immunohistochemical staining of Ly6G in the colon on day 7 after colitis induction. Scale bar = 100 μ m. (B) Representative FACS plots for Ly6G staining gated on NEs isolated from mice colon. The ratios of Ly6G-positive cells are shown. (C) Grouping of NE migration experiments using the transwell system with 8-micron pore size. (D) NE migration and enumeration through pores. (E) Grouping of experiments using the caco-2 monolayer model using the transwell system with 0.4-micron pore size. (F) Caco-2 cells were plated on a permeable membrane for TEER at different time points. (G) FITC-dextran flux was measured using caco-2 cells grown to maximum TEER. * $p < 0.05$, ** $p < 0.01$, *** $p < 0.001$. All experiments in vitro were repeated three times. All data are presented as mean \pm SD.

Abbreviation: TEER, transepithelial electrical resistance.

TLR2/ERK Pathway Mediated IECs IL-8 secretion by *F. Nucleatum* Infection

To investigate the intercellular pathways for *F. nucleatum*-induced IL-8 secretion from IEC, we performed transcriptome analysis, and the KEGG analysis revealed that the “Toll-like receptor signaling pathway”, “MAPK signaling pathway” and “NF-kappaB signaling pathway” were enriched (Figure 5A). Considering that TLRs signaling is significant for *F. nucleatum*-induced pathogenesis and that the role of the TLR2/ERK signaling pathway in IL-8 secretion has been reported, we hypothesized that *F. nucleatum* promotes epithelial cells to secrete IL-8 by upregulating the TLR2/ERK signaling pathway. We found that TLR2 and p-ERK were upregulated in *F. nucleatum*-infected IEC lines (Figure 5B). In addition, the expression of TLR2 was also up-regulated in mouse colon tissue after infection with *F. nucleatum* (Figure 5C). To confirm the necessity of TLR2/ERK for improving IL-8 secretion, we used an inhibitor of the TLR2/ERK signaling pathway. Following the application of TLR2 inhibitor C29, the increase in IL-8 transcription and secretion levels induced by *F. nucleatum* was significantly reduced (Figure 5D and E). Meanwhile, C29 decreased the expression level of TLR2 protein and the phosphorylation level of ERK induced by *F. nucleatum* infection (Figure 5F). Next, we used the ERK inhibitor U0126 and found that both the secretion and transcription levels of IL-8 decreased (Figure 5G and H). These results indicated that *F. nucleatum* promotes IL-8 secretion via the TLR2/ERK pathway.

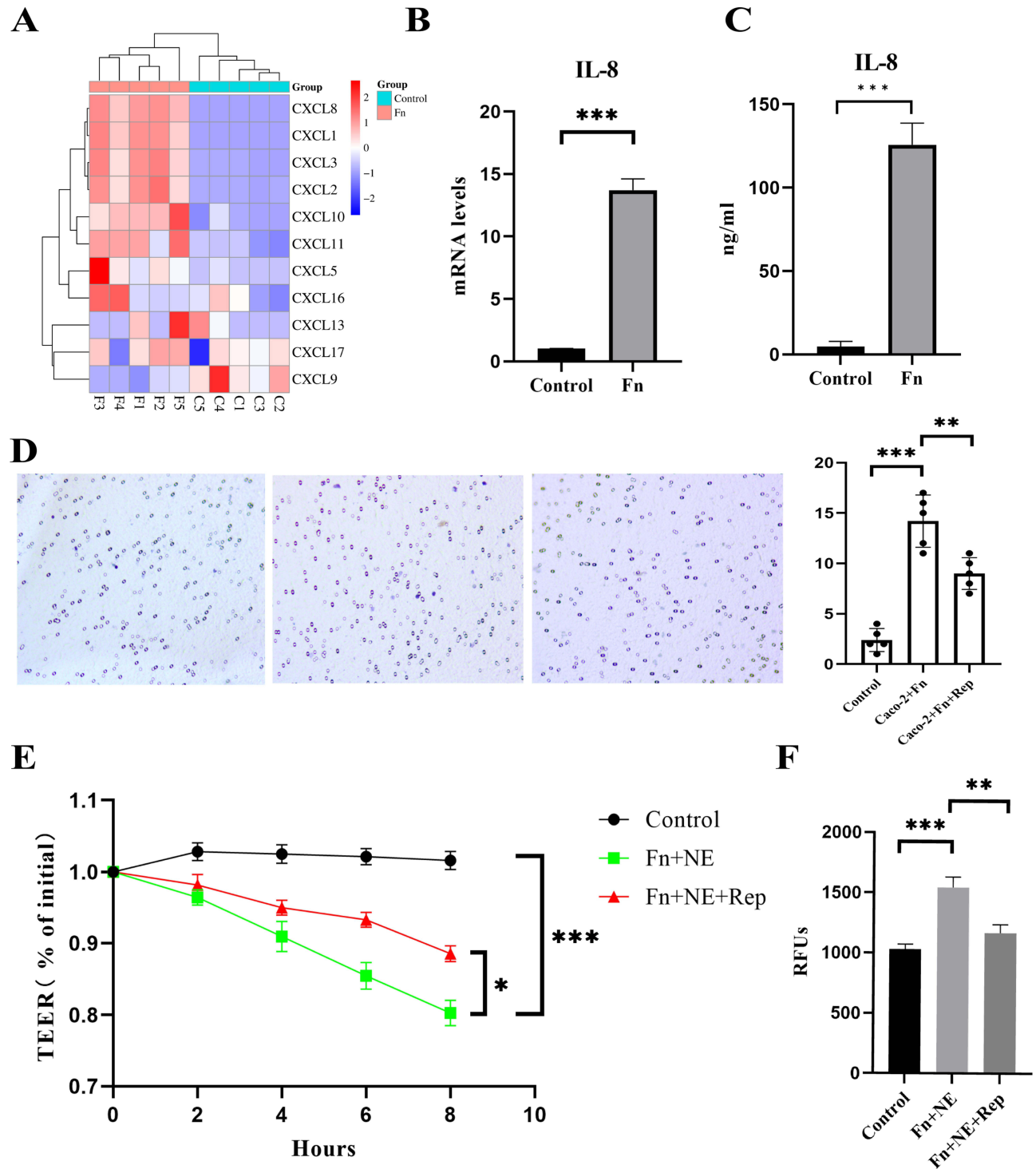


Figure 4 Epithelial cells were activated by *F. nucleatum* to secrete IL-8 and then recruiting neutrophils. **(A)** Revelations of gene expression alterations in caco-2 cells induced by *F. nucleatum* infection unveiled through sequencing. **(B)** The mRNA levels of IL-8 by caco-2 cells were assessed using RT-qPCR. **(C)** The secretion levels of IL-8 by caco-2 cells were assessed using ELISA. **(D)** Following treatment with Reparixin, NE migration, and enumeration through pores. **(E)** Following treatment with Reparixin, Caco-2 cells were plated on a permeable membrane for TEER at different time points. **(F)** Following treatment with Reparixin, FITC-dextran flux was measured after Caco-2 cells were grown to maximum TEER. * $p < 0.05$, ** $p < 0.01$, *** $p < 0.001$. All experiments in vitro were repeated three times. All data are presented as mean \pm SD. **Abbreviation:** TEER, transepithelial electrical resistance.

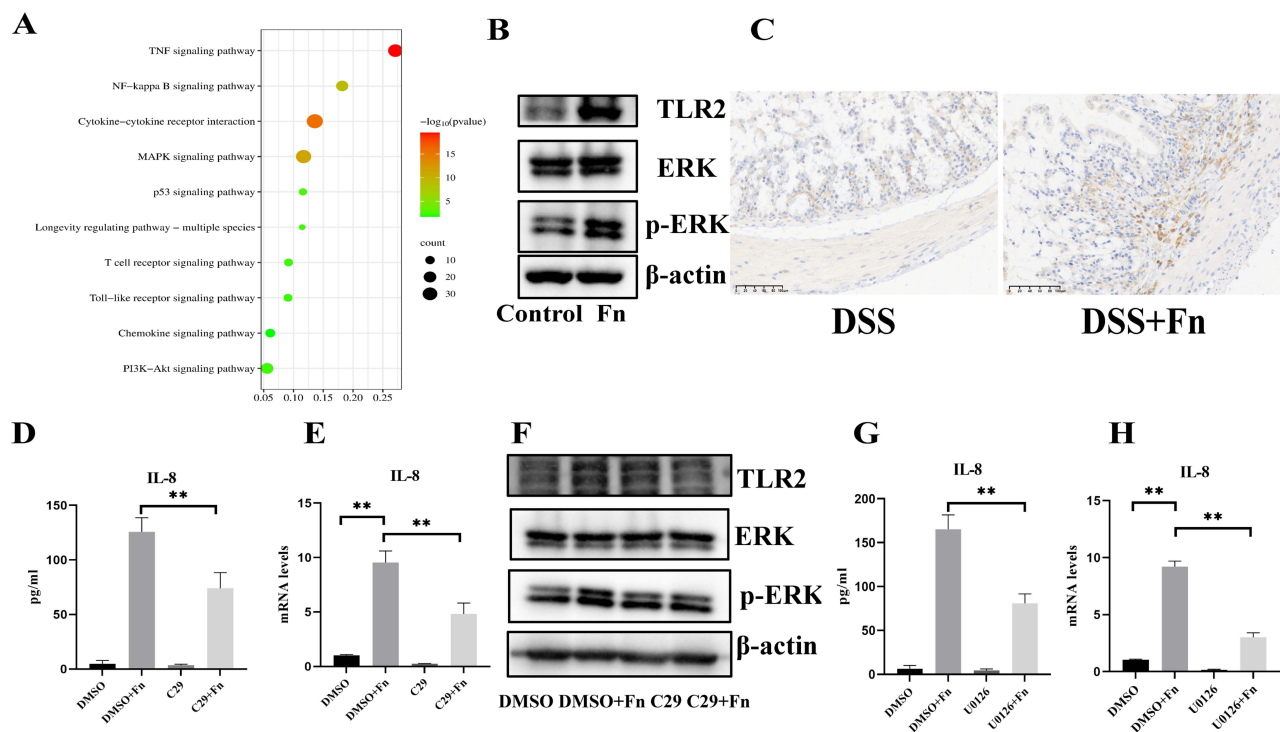


Figure 5 TLR2/ERK pathway mediated IECs IL-8 secretion by *F. nucleatum* infection. **(A)** KEGG analysis was conducted to show the altered gene sets expression of caco-2 cells induced by *F. nucleatum* infection. **(B)** Immunoblot analysis of protein extracts from caco-2 samples with the indicated antibodies. **(C)** Representative images of immunohistochemical staining of TLR-2 in the colon on day 7 after colitis induction. Scale bar = 100 μ m. **(D)** The IL-8 secretion levels from caco-2 cells were assessed via ELISA following treatment with C29. **(E)** The IL-8 mRNA levels from caco-2 cells were assessed via RT-qPCR following treatment with C29. **(F)** Following treatment with C29, protein extracts from caco-2 cells were subjected to immunoblot analysis using the specified antibodies. **(G)** The IL-8 secretion levels from caco-2 cells were assessed via ELISA following treatment with U0126. **(H)** The IL-8 mRNA levels from caco-2 cells were assessed via RT-qPCR following treatment with U0126. ** $p < 0.01$. All experiments in vitro were repeated three times. All data are presented as mean \pm SD.

Neutrophil Exhaustion Restored *F. Nucleatum*-Induced Intestinal Barrier Impairment and Mucosa Inflammation

NEs are essential for *F. nucleatum*-induced intestinal barrier impairment and mucosal inflammation. We applied the NE exhaustion mouse model by anti-Ly6G intraperitoneal injection and confirmed that the model was sufficient for further study by examining the spleen NEs (Figure 6A). We found that mice with NE exhaustion had a lower NE proportion, even after *F. nucleatum* treatment (Figure 6B). In addition, NE-exhausting mice exhibited a milder colitis pathology (Figure 6C–E). We further found that NE exhaustion relieved intestinal barrier dysfunction, including intestinal permeability and tight junction protein expression (Figure 6F and G). These results indicate that *F. nucleatum*-induced NEs contribute to intestinal barrier impairment and inflammation.

Discussion

In the present study, we demonstrated that *F. nucleatum* aggravated DSS-induced colitis by improving NE chemotaxis. *F. nucleatum* can infect epithelial cells and secrete IL-8 via the TLR2/ERK signaling pathway, which induces NE chemotaxis. NE-induced intestinal barrier impairment may contribute to colitis development and progression. The findings of this study highlight the crucial role of *F. nucleatum*-mediated NEs in the regulation of the intestinal barrier defense. Furthermore, this study suggested that targeting *F. nucleatum* infection could be a potential approach to mitigate intestinal inflammation and prevent barrier impairment in colitis.

In the late 1980s, one study suggested a close connection between the microbiota and NEs.¹¹ Further studies have shown that the intestinal microbiota can affect the production, chemotaxis, activation, and differentiation of NEs.¹² *F. nucleatum*, which has been extensively implicated in colorectal cancer studies, is tightly linked with IBD development in recent studies.^{3,4} A study has shown that *F. nucleatum* is enriched in the intestines of patients with ulcerative colitis

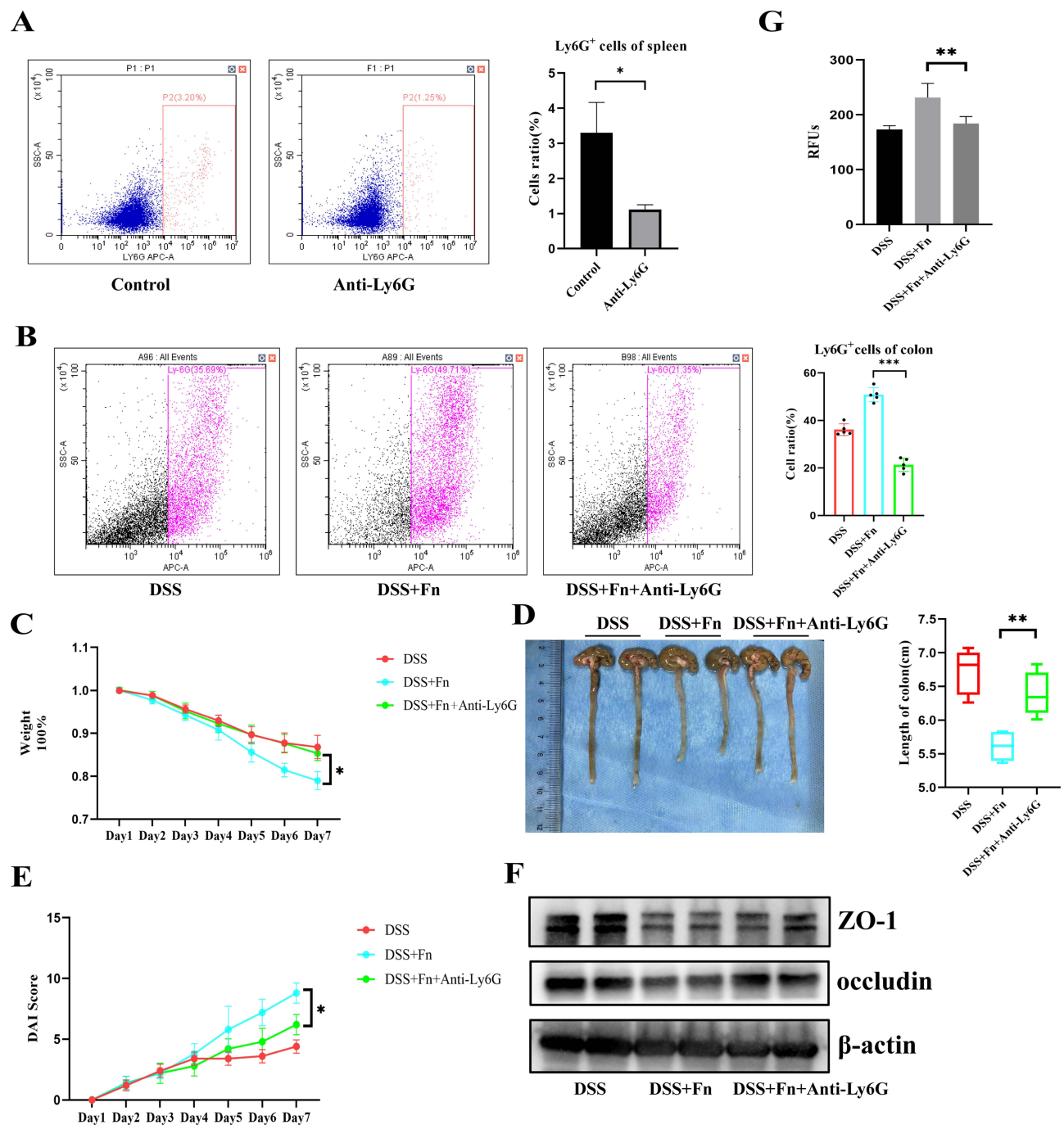


Figure 6 Neutrophil exhaustion restored *F. nucleatum*-induced intestinal barrier impairment and mucosa inflammation. **(A)** Representative FACS plots for Ly6G staining gated on NEs isolated from mice spleen. The ratios of Ly6G-positive cells are shown. (n = 3 mice per group) **(B)** Representative FACS plots for Ly6G staining gated on NEs isolated from mice colon. The ratios of Ly6G-positive cells are shown. (n = 5 mice per group) **(C)** Effect on body weight of mice. (n = 5 mice per group). **(D)** A Photograph of the representative colon, and colon length was measured on day 7 after colitis induction. (n = 5 mice per group) **(E)** Clinical DAI assessed after colitis treatment. (n = 5 mice per group) **(F)** Immunoblot analysis of protein extracts from the colon samples using the indicated antibodies. **(G)** Relative fluorescence intensity of FITC-Dextran 4KDa in blood 2 h after oral administration of FD4. (n = 5 mice per group) * $p < 0.05$, ** $p < 0.01$, *** $p < 0.001$. All data are presented as mean \pm SD.

and exacerbates colitis by activating autophagy in intestinal epithelial cells.¹³ Not only can *F. nucleatum* directly act on epithelial cells to exacerbate colitis, but it can also modulate immune cells to influence inflammation. A recent study has shown that *F. nucleatum* can promote the development of intestinal inflammation and aggravate colitis by mediating M1 macrophages.¹⁴ Another study showed that macrophage polarization triggered by *F. nucleatum* leads to IEC apoptosis

and promotes colitis progression of colitis.¹⁵ These studies suggest that *F. nucleatum* is related to inflammatory cells and explore the role of interactions between epithelial cells and lamina propria immune cells.

Our results reveal that *F. nucleatum* infects epithelial cells, causing them to secrete IL-8 and induce NE chemotaxis. This is consistent with some studies showing that *F. nucleatum* promotes IL-8 secretion in colitis-associated cancer microenvironment.¹⁶ We performed transcriptome analysis of *F. nucleatum*-infected epithelial cells and found that IL-8 levels showed the most significant increase, as confirmed by ELISA. IL-8 is an important cytokine that activates NEs in various diseases.^{17–19} IL-8 also activates NEs and induces the production of superoxide.²⁰ In the present study, we found that NE chemotaxis and function mainly depend on the secretion of IL-8 by epithelial cells. However, inflammatory epithelial cells release other cytokines to enable neutrophil migration to sites of inflammation, such as IL-6, IL-1 β .²¹ It is widely accepted that IL-8, the most effective cytokine released by epithelial cells, attracts NEs to the basolateral surface of the epithelium.²¹

As is widely recognized, the intestinal barrier serves as a physical barrier that prevents invasion of intestinal contents.²² Impairment of the epithelial barrier increases the permeability of the intestinal mucosa, facilitating contact of intestinal luminal materials with deep structures and causing subsequent damage. We found that *F. nucleatum* reduced the integrity of the caco-2 monolayer and increased its permeability of the caco-2 monolayer after co-culturing with NEs in vitro. In addition, *F. nucleatum* increased the intestinal permeability of caco-2 monolayer. These results suggest *F. nucleatum* impairs barrier integrity and upregulates barrier permeability by activating the NEs. Impaired integrity and abnormal permeability of the intestinal barrier can facilitate the entry of enteric pathogens and luminal toxins into intestinal tissue, aggravating colitis.

NEs have been increasingly recognized as having dual functions in IBD. NEs secrete bactericidal components, prevent the spread of microorganisms, and facilitate mucosal healing following intestinal injury. This contributes to maintaining the stability of the intestinal barrier.^{23,24} A recent study found that a subset of NEs can secrete IL-22 to protect barrier function.²⁵ Conversely, excessive NE activity can compromise intestinal barrier function, damage the intestinal epithelium, and exacerbate disease symptoms.²⁶ NEs directly promote tissue damage by releasing proteins such as MMPs and NE elastase as well as by releasing reactive oxygen species (ROS) to alter the properties of the cell membrane.^{27–29} We found that NE exhaustion could reduce inflammation and restore intestinal barrier function in DSS-induced mice with *F. nucleatum* infection.

Toll-like receptors (TLRs) play a crucial role in sensing pathogen-associated molecular patterns (PAMPs).³⁰ TLR2 is a type I pattern-recognition receptor that participates in intestinal homeostasis.³¹ A previous study revealed that TLR2 and TLR4 play critical roles in intestinal inflammation caused by *F. nucleatum* infection.³² TLR2 activation is positively correlated with colitis activity.^{33–35} By sequencing the transcriptome, we confirmed that *F. nucleatum* can activate the TLR2/ERK signaling pathway, which is often activated and plays an essential role in cytokine production.^{36,37} Epithelial cells secrete inflammatory cytokines that induce NE chemotaxis by activating TLR2/ERK, aggravating colitis.

From a clinical perspective, antimicrobial therapy is a potential therapeutic approach for IBD, aiming to inhibit pathogenetic bacteria such as *F. nucleatum*. Meanwhile, probiotics and metabolites could offer new treatments for intestinal inflammation without disrupting the overall structure of the intestinal microbiota. A study revealed fucose can influence the metabolism of *F. nucleatum* and reduce intestinal inflammation.³⁸ Another study has demonstrated the potential of *Akkermansia Muciniphila* to inhibit inflammation caused by *F. nucleatum*.³⁹ In addition, targeting cytokines is another potential therapeutic strategy. A study on the alleviation of colitis caused by *F. nucleatum* infection through the neutralization of IL-1 α .⁴⁰ IL-8-CXCR1/2 signaling can be another potential target for the treatment of IBD, similar to the IL-12/23 inhibitors currently in use and the CXCR4 blockers that are under development.

This study demonstrates that *F. nucleatum* infects epithelial cells and induces NE chemotaxis. However, this study had some limitations. We did not explore the direct effects of *F. nucleatum* on NEs. However, previous research consistent with our experiment showed that the secretion of IL-8 is dependent on infection of other cells by *F. nucleatum*.⁴¹ NE exhaustion model is an in vivo method used to explore the role of NEs in disease models.⁴² It is challenging to screen for NE subtypes with distinct functions instead of total NE exhaustion. However, we found that

F. nucleatum plays a crucial role in promoting NE chemotaxis and is integral to regulating cytokine secretion by epithelial cells.

Conclusion

In summary, our results suggest that during inflammation in colitis, *F. nucleatum* infects epithelial cells and induces NE chemotaxis by secreting IL-8. Preventing the progression of IBD by eliminating *F. nucleatum* or blocking downstream signaling pathways could be therapeutic targets for future studies.

Author Contributions

All authors made a significant contribution to the work reported, whether that is in the conception, study design, execution, acquisition of data, analysis and interpretation, or in all these areas; took part in drafting, revising or critically reviewing the article; gave final approval of the version to be published; have agreed on the journal to which the article has been submitted; and agree to be accountable for all aspects of the work.

Funding

This research was supported by the Natural Science Foundation of China (Grant No. 82300631), Ningbo Top Medical and Health Research Program (Grant No. 2022010101), Zhejiang Provincial Natural Science Foundation of China (Grant No. Q23H030003), and Ningbo Public Service Technology Foundation (Grant No. 2023J405).

Disclosure

The authors have claimed that there was no competing interest related to this study.

References

1. Kobayashi T, Siegmund B, Le Berre C, et al. Ulcerative colitis. *Nat Rev Dis Prim.* 2020;6(1):74. doi:10.1038/s41572-020-0205-x
2. Roda G, Chien Ng S, Kotze PG, et al. Crohn's disease. *Nat Rev Dis Prim.* 2020;6(1):22. doi:10.1038/s41572-020-0156-2
3. Huh JW, Roh TY. Opportunistic detection of Fusobacterium nucleatum as a marker for the early gut microbial dysbiosis. *BMC Microbiol.* 2020;20(1):208. doi:10.1186/s12866-020-01887-4
4. Strauss J, Kaplan GG, Beck PL, et al. Invasive potential of gut mucosa-derived Fusobacterium nucleatum positively correlates with IBD status of the host. *Infl bowel dis.* 2011;17(9):1971–1978. doi:10.1002/ibd.21606
5. Cao P, Chen Y, Guo X, et al. Fusobacterium nucleatum activates endoplasmic reticulum stress to promote crohn's disease development via the upregulation of CARD3 expression. *Front Pharmacol.* 2020;11:106. doi:10.3389/fphar.2020.00106
6. Phillipson M, Kubes P. The healing power of neutrophils. *Trends in Immunol.* 2019;40(7):635–647. doi:10.1016/j.it.2019.05.001
7. Danne C, Skerniskyte J, Marteyn B, Sokol H. Neutrophils: from IBD to the gut microbiota. *Nat Rev Gastroenterol Hepatol.* 2023;21: 184–97.
8. Kong X, Zhang Y, Xiang L, et al. Fusobacterium nucleatum-triggered neutrophil extracellular traps facilitate colorectal carcinoma progression. *J Exp Clin Cancer Res.* 2023;42(1):236. doi:10.1186/s13046-023-02817-8
9. Vlantis K, Polykratis A, Welz PS, van Loo G, Pasparakis M, Wullaert A. TLR-independent anti-inflammatory function of intestinal epithelial TRAF6 signalling prevents DSS-induced colitis in mice. *Gut.* 2016;65(6):935–943. doi:10.1136/gutjnl-2014-308323
10. Shi S, Liu Y, Wang Z, et al. Fusobacterium nucleatum induces colon anastomosis leak by activating epithelial cells to express MMP9. *Front Microbiol.* 2022;13:1031882. doi:10.3389/fmicb.2022.1031882
11. Neffel KA, Hauser SP, Müller MR. Inhibition of granulopoiesis in vivo and in vitro by beta-lactam antibiotics. *J Infect Dis.* 1985;152(1):90–98. doi:10.1093/infdis/152.1.90
12. Smith CK, Trinchieri G. The interplay between neutrophils and microbiota in cancer. *J Leukocyte Biol.* 2018;104(4):701–715. doi:10.1002/JLB.4RI0418-151R
13. Su W, Chen Y, Cao P, et al. Fusobacterium nucleatum promotes the development of ulcerative colitis by inducing the autophagic cell death of intestinal epithelial. *Front Cell Infect Microbiol.* 2020;10:594806. doi:10.3389/fcimb.2020.594806
14. Liu L, Liang L, Liang H, et al. Fusobacterium nucleatum aggravates the progression of colitis by regulating M1 macrophage polarization via AKT2 pathway. *Front Immunol.* 2019;10:1324. doi:10.3389/fimmu.2019.01324
15. Liu L, Liang L, Yang C, Zhou Y, Chen Y. Extracellular vesicles of Fusobacterium nucleatum compromise intestinal barrier through targeting RIPK1-mediated cell death pathway. *Gut Microbes.* 2021;13(1):1–20. doi:10.1080/19490976.2021.1902718
16. AD K, Chun E, Robertson L, et al. Fusobacterium nucleatum potentiates intestinal tumorigenesis and modulates the tumor-immune microenvironment. *Cell Host Microbe.* 2013;14(2):207–215. doi:10.1016/j.chom.2013.07.007
17. Godaly G, Proudfoot AE, Offord RE, Svanborg C, Agace WW. Role of epithelial interleukin-8 (IL-8) and neutrophil IL-8 receptor A in Escherichia coli-induced transuroepithelial neutrophil migration. *Infect Immun.* 1997;65(8):3451–3456. doi:10.1128/iai.65.8.3451-3456.1997
18. Allen TC, Kurdowska A. Interleukin 8 and acute lung injury. *Arch Pathol Lab Med.* 2014;138(2):266–269. doi:10.5858/arpa.2013-0182-RA
19. Harada A, Sekido N, Akahoshi T, Wada T, Mukaida N, Matsushima K. Essential involvement of interleukin-8 (IL-8) in acute inflammation. *J Leukocyte Biol.* 1994;56(5):559–564. doi:10.1002/jlb.56.5.559
20. Matsushima K, Yang D, Oppenheim JJ. Interleukin-8: an evolving chemokine. *Cytokine.* 2022;153:155828. doi:10.1016/j.cyto.2022.155828

21. Kang L, Fang X, Song YH, et al.: Neutrophil-epithelial crosstalk during intestinal inflammation. *Cell mol gastroenterol hepatol* 2022, 14 (6):1257–1267.
22. Liu H, Hong XL, Sun TT, Huang XW, Wang JL, Xiong H. Fusobacterium nucleatum exacerbates colitis by damaging epithelial barriers and inducing aberrant inflammation. *J Dig Dis*. 2020;21(7):385–398. doi:10.1111/1751-2980.12909
23. Garrido-Trigo A, AM C, Veny M, et al. Macrophage and neutrophil heterogeneity at single-cell spatial resolution in human inflammatory bowel disease. *Nat Commun*. 2023;14(1):4506. doi:10.1038/s41467-023-40156-6
24. Isles HM, Herman KD, Robertson AL, et al. The CXCL12/CXCR4 signaling axis retains neutrophils at inflammatory sites in zebrafish. *Front Immunol*. 2019;10:1784. doi:10.3389/fimmu.2019.01784
25. Zhou G, Yu L, Fang L, et al. CD177(+) neutrophils as functionally activated neutrophils negatively regulate IBD. *Gut*. 2018;67(6):1052–1063. doi:10.1136/gutjnl-2016-313535
26. Ballesteros I, Rubio-Ponce A, Genua M, et al. Co-option of neutrophil fates by tissue environments. *Cell*. 2020;183(5):1282–1297.e1218. doi:10.1016/j.cell.2020.10.003
27. de Bruyn M, Vandooren J, Ugarte-Berzal E, Arijis I, Vermeire S, Opendakker G. The molecular biology of matrix metalloproteinases and tissue inhibitors of metalloproteinases in inflammatory bowel diseases. *Crit Rev Biochem Mol Biol*. 2016;51(5):295–358. doi:10.1080/10409238.2016.1199535
28. Barry R, Ruano-Gallego D, ST R, et al. Faecal neutrophil elastase-antiprotease balance reflects colitis severity. *Mucosal Immunol*. 2020;13 (2):322–333. doi:10.1038/s41385-019-0235-4
29. Lu H, Lin J, Xu C, et al. Cyclosporine modulates neutrophil functions via the SIRT6-HIF-1 α -glycolysis axis to alleviate severe ulcerative colitis. *Clinic Transl Med*. 2021;11(2):e334. doi:10.1002/ctm2.334
30. Lim KH, Staudt LM. Toll-like receptor signaling. *Cold Spring Harbor Perspect Biol*. 2013;5(1):a011247. doi:10.1101/cshperspect.a011247
31. Candia E, Díaz-Jiménez D, Langjahr P, et al. Increased production of soluble TLR2 by lamina propria mononuclear cells from ulcerative colitis patients. *Immunobiology*. 2012;217(6):634–642. doi:10.1016/j.imbio.2011.10.023
32. Jia YP, Wang K, Zhang ZJ, et al. TLR2/TLR4 activation induces Tregs and suppresses intestinal inflammation caused by Fusobacterium nucleatum in vivo. *PLoS One*. 2017;12(10):e0186179. doi:10.1371/journal.pone.0186179
33. Wang L, Gong Z, Zhang X, et al. Gut microbial bile acid metabolite skews macrophage polarization and contributes to high-fat diet-induced colonic inflammation. *Gut Microbes*. 2020;12(1):1–20. doi:10.1080/19490976.2020.1819155
34. Shmuel-Galia L, Aychek T, Fink A, et al. Neutralization of pro-inflammatory monocytes by targeting TLR2 dimerization ameliorates colitis. *EMBO J*. 2016;35(6):685–698. doi:10.15252/embj.201592649
35. Li J, Bai J, Song Z, et al. Dietary pectin attenuates Salmonella typhimurium-induced colitis by modulating the TLR2-NF- κ B pathway and intestinal microbiota in mice. *Food Chem Toxicol*. 2023;182:114100. doi:10.1016/j.ftc.2023.114100
36. SR P, DJ K, SH H, et al. Diverse Toll-like receptors mediate cytokine production by Fusobacterium nucleatum and Aggregatibacter actinomyces-temcomitans in macrophages. *Infect Immun*. 2014;82(5):1914–1920. doi:10.1128/IAI.01226-13
37. Chang YR, Cheng WC, Hsiao YC, et al. Links between oral microbiome and insulin resistance: involvement of MAP kinase signaling pathway. *Biochimie*. 2023;214(Pt B):134–144. doi:10.1016/j.biochi.2023.06.013
38. Duan C, Hou L, Deng X, et al. Fucose ameliorates the proinflammatory property of Fusobacterium nucleatum in colitis via altering its metabolism. *Front Cell Infect Microbiol*. 2023;13:1190602. doi:10.3389/fcimb.2023.1190602
39. Song B, Xian W, Sun Y, et al. Akkermansia muciniphila inhibited the periodontitis caused by Fusobacterium nucleatum. *NPJ biofilms microbiomes*. 2023;9(1):49. doi:10.1038/s41522-023-00417-0
40. Boonyaleka K, Okano T, Iida T, et al. Fusobacterium nucleatum infection activates the noncanonical inflammasome and exacerbates inflammatory response in DSS-induced colitis. *European j Immunol*. 2023;53(11):e2350455. doi:10.1002/eji.202350455
41. MA C, CC Y, Udayasuryan B, et al. Fusobacterium nucleatum host-cell binding and invasion induces IL-8 and CXCL1 secretion that drives colorectal cancer cell migration. *Sci Signaling*. 2020;13(641). doi:10.1126/scisignal.aba9157.
42. Boivin G, Faget J, PB A, et al. Durable and controlled depletion of neutrophils in mice. *Nat Commun*. 2020;11(1):2762. doi:10.1038/s41467-020-16596-9

Journal of Inflammation Research

Dovepress

Publish your work in this journal

The Journal of Inflammation Research is an international, peer-reviewed open-access journal that welcomes laboratory and clinical findings on the molecular basis, cell biology and pharmacology of inflammation including original research, reviews, symposium reports, hypothesis formation and commentaries on: acute/chronic inflammation; mediators of inflammation; cellular processes; molecular mechanisms; pharmacology and novel anti-inflammatory drugs; clinical conditions involving inflammation. The manuscript management system is completely online and includes a very quick and fair peer-review system. Visit <http://www.dovepress.com/testimonials.php> to read real quotes from published authors.

Submit your manuscript here: <https://www.dovepress.com/journal-of-inflammation-research-journal>